Design and Implementation of an Intelligent Analgesic Bracelet Based on Wrist-ankle Acupuncture

Ping Shi, Jiahao Du, Fanfu Fang, Hongliu Yu, and Junwen Liu

***Abstract*—A flexible, multifunctional, and intelligent analgesic bracelet was proposed in this article to alleviate symptoms of pain. Based on the theory of wrist-ankle acupuncture in traditional Chinese medicine, transcutaneous electrical nerve stimulation is the technical basis of the method. A set of targeted circuit system capable of generating adjustable electrical stimulation signals to simulate filamentary acupuncture was designed. The system architecture includes a wireless communication module, a signal control module, a stimulus signal generation module, and a wearable, flexible bracelet. In addition, a pain assessment interface with a visual analog scale was designed to assess pain levels. Two comparative experiments were designed, involving a custom pain assessment scale and hand-held dolorimeter that were performed before and after wearing the bracelet to verify the analgesic effect of the bracelet. The results showed that the wrist-worn analgesic bracelet is significantly effective in alleviating pain in various parts of the human body.**

***Index Terms*—Analgesic, circuit system, pain assessment, transcutaneous electrical nerve stimulation (TENS), wrist-ankle acupuncture (WAA).**

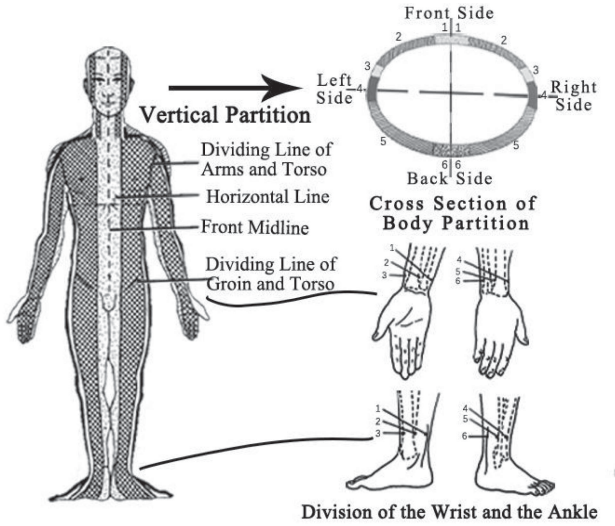

Fig. 1. Schematic diagram of WAA partition.

I. Introduction

CHRONIC pain is a highly prevalent and debilitating condition, and there is a pressing need to find safe, effective, convenient, and affordable treatments to address this public health issue [1], [2]. The substantial number of people suffering from pain, the tremendous medical costs, and the negative impact of pain on quality of life are all reasons why the treatment of chronic pain deserves attention [3].

Clinical methods of analgesia mainly include prescription drugs [4]. Opioids have a strong analgesic effect and have been used as the primary treatment of chronic pain [5]. However, they also reduce central respiratory drive and the sensitivity of the cough reflex and cause nausea, vomiting, constipation, and mental impairment. These undesirable effects delay the recovery of patients and prolong the length of hospital stay. In addition, a great number of studies on nonpharmacological methods of analgesia such as acupuncture and transcutaneous electrical nerve stimulation (TENS) have indicated an apparent reduction in pain sensation of patients after treatment [6]–[9]. Acupuncture, which has been practiced for over 2000 years in China, has been extensively used for the treatment of pain outside China, especially after the release of the National Institutes of Health (NIH) Consensus in 1997 [10]–[12]. It is a useful complementary therapy due to its ease of application, relative safety, and lack of evident systemic side effects. However, it is limited by its cost, patient scheduling difficulties, and invasive therapy. During this period, great efforts have been made to realize an effective analgesia system combined with the noninvasive technique, such as Han's acupoint nerve stimulator (HANS) [13], the 64-independent channel stimulator (ShefStim-SBS) [14], and the transcutaneous electrical nerve stimulator (DX66053) [15]. These devices are based on TENS and have shown significant efficacy in controlling postoperative pain after various procedures, including cardiac surgeries [16], cholecystectomy [17], cesarean section [18], liposuction [19],

Manuscript received August 6, 2020; revised September 29, 2020; accepted November 4, 2020. Date of publication November 18, 2020; date of current version December 30, 2020. This work was supported in part by the National Key R&D Program of China under Grant 2019YFC1711800, in part by the Action Plan for Scientific and Technological Innovation under Grant 19441901300, and in part by the Action Plan for Scientific and Technological Innovation under Grant 19441908100. *(Corresponding author: Fanfu Fang.)*

Ping Shi, Jiahao Du, Hongliu Yu, and Junwen Liu are with the Department of Rehabilitation Engineering, University of Shanghai for Science and Technology, Shanghai 200093, China (e-mail: togethershi@163.com; ddujh@qq.com; yhl98@hotmail.com; chengwen712@126.com).

Fanfu Fang is with the Department of Rehabilitation Medicine, Changhai Hospital of Traditional Chinese Medicine, Naval Medical University, Shanghai 200433, China (e-mail: fangfanfu@126.com).

Color versions of one or more figures in this article are available at https://doi.org/10.1109/TBCAS.2020.3039063.

Digital Object Identifier 10.1109/TBCAS.2020.3039063

total knee arthroplasty [20], and thoracotomy [21]. The analgesic effects of TENS are reportedly produced via the activation of opioid receptors [22]–[24], descending pain modulation, and segmental pain inhibition [25]. Most TENS devices can be used essentially anywhere on the body for stimulation through individually wired electrodes, which are placed near the site of pain on the patients' body [26]–[29]. However, most of these devices are bulky and nonportable, and the electrodes are placed in disorder and unfocused. Additionally, wired electrodes are also troublesome in daily activities and sleep. Therefore, there is a special need to develop a portable, compact, and wearable wireless TENS device.

As an alternative, TENS based on the wrist-ankle acupuncture (WAA) theory may be useful. WAA is a modern subcutaneous acupuncture technique that was invented and developed by Professor Zhang Xinshu and his colleagues from the Changhai Hospital of Second Military Medical University in Shanghai, China, in the 1970s [30]. Different from traditional acupuncture, WAA is superficial acupuncture that is applied on the specific area of the wrist or the ankle corresponding to the site of pain area, where there are no crucial organs or vessels, to treat a range of pain symptoms throughout the body, as shown in Fig. 1 [31]. WAA divides the body into six longitudinal zones. There are six zones and needle entry points on the left and right wrists and ankles respectively. The wrist part is upper zone 1, upper zone 2, …, upper zone 6, and the left and right hands are symmetrical. The ankle part is inferior zone 1, zone 2, …, zone 6, symmetrical left and right. Superficial subcutaneous puncture in different zones and needle insertion points can treat the pain of the corresponding tissue organs. In accordance with the unique theory on which WAA is based, clinical evidence has shown that WAA can relieve both chronic and acute pain [32], [33].

In WAA, the functions of corresponding meridians and viscera are adjusted by the stimulation of cutaneous regions, allowing the blood to circulate without obstruction. It is believed that "there is no pain when the circulation of Qi and blood is unobstructed." Moreover, another animal study showed that the analgesic mechanism of WAA is related to neurohumoral regulation [34]. Hence, WAA is a relatively safe, convenient, and quick procedure, which requires only the precise identification of needle locations appropriate for the patients' signs and symptoms [35]. Nonetheless, invasive acupuncture technology can be implemented only by professional physicians, as it is challenging to perform at home. Consequently, it is necessary to design a noninvasive and effective analgesic device for patients at home.

In this paper, we developed an intelligent analgesic bracelet that is worn on the wrist or the ankle and stimulates the corresponding area of the wrist or the ankle to relieve pain by simulating the pulse wave targeted in acupuncture, as shown in Fig. 2. This smart bracelet combines the WAA theory with TENS treatment, and uses electrical stimulation to simulate the effect of WAA, which reduces the inconvenience of TENS treatment and eliminates the concerns of patients for invasive treatment. The analgesic effect of TENS is intimately related to the parameter setting, including pulse intensity, pulse frequency, and stimulation site. The particular analgesic circuit designed in this paper can realize the pulse wave of analog acupuncture with an adjustable intensity of 0-100 V and frequency of 0-100 Hz. These pulses are applied to corresponding acupuncture points on the human body through the gold electrodes embedded inside the bracelet. The specific stimulation points were guided by WAA. In addition, a customized pain assessment scale was designed to evaluate the analgesic effect of the bracelet through two sets of comparative experiments. The experimental results demonstrated that the intelligent analgesic bracelet performs well in analgesic experiments and is a feasible treatment for pain relief.

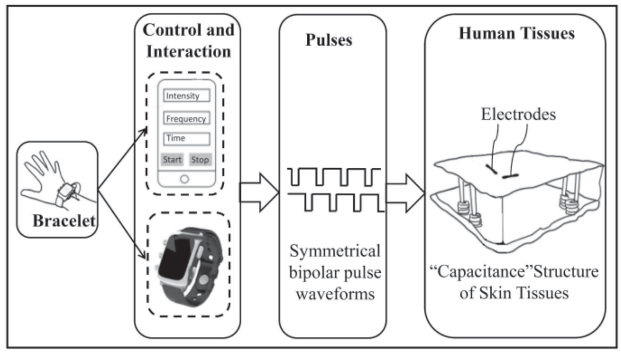

Fig. 2. Operating mechanism of the intelligent bracelet.

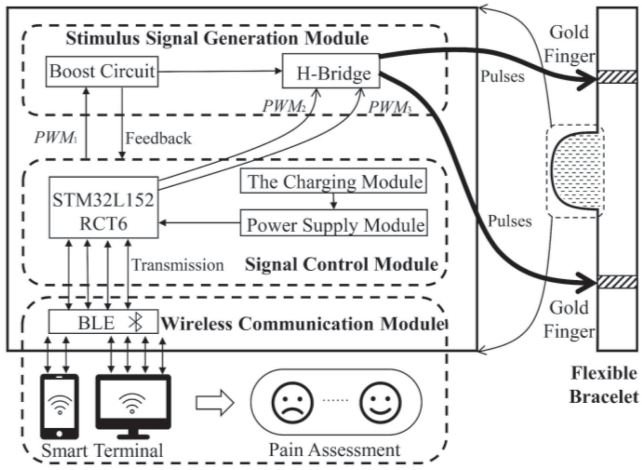

Fig. 3. System architecture of the proposed intelligent analgesic bracelet design.

II. System Architecture

The intelligent analgesic bracelet mainly regulates the number of motor units recruited and the emissivity of muscle fibers by adjusting the intensity and frequency of stimulation, and produce an analgesic effect on the human body. The stimulation intensity is controlled by voltage or current.

The system architecture of the proposed smart analgesic bracelet is shown in Fig. 3. The users set the analgesic parameters (intensity, frequency, and time) through the intelligent terminal, and the wireless communication module decodes the parameters

and transmits them to the signal control module. The signal control module receives, demodulates, and processes the signals to generate adjustable electrical stimulation pulses. Then the electrical stimulation pulses stimulate the corresponding area of the wrist or the ankle through a pair of gold electrodes embedded in the flexible bracelet. The electrical stimulation pulses use symmetrical bipolar pulse waveforms, which can reduce the polarization response during pain treatment and prevent skin damage [36]. The proposed architecture is fully integrated and highly scalable, and it can be scaled without compromising analgesic performance.

In the present paper, a voltage mode stimulation was adopted. Specifically, it was more efficient to use a voltage-mode stimulation in high-current stimulators (such as pacemakers and spinal cord stimulators) compared to current mode stimulation [37]. The setting of the voltage index is related to the safety current passing through the human body, the skin impedance of the human body, and the tolerance of the patients' acupuncture site. The safe current that the human body can withstand in most cases is 10 mA. When the current intensity reaches 50 mA, apnea and ventricular fibrillation caused by paralysis will cause the human body to enter a coma state or possibly die. Since this design is used to treat patients with pain, to ensure the safety of patients receiving treatment, the current through the human body should be 10-50 mA. The impedance of human skin in the frequency range 0 to 100 Hz is 1.0-3.5KΩ [38]. Moreover, a voltage above 80 V can conduct effective current through the skin. Considering the actual influencing factors, such as the tube consumption, the resistance consumption, the stability of the circuit, and the stability of the patients, the maximum output voltage of the treatment designed is 100 V, which is in the safety category.

TENS stimulation at different frequencies can produce analgesic effects, but the analgesic substances released by the central nervous system are different. The stimulation frequency of the bracelet can be widely adjusted according to the purpose of the research or the specific condition. Some studies have indicated that the optimal frequency of most mammalian muscles and nerves does not exceed 100 Hz [39]. The analog frequency of 100Hz has the function of the calming central nervous system and curing or relieving pain. Low-frequency pulsed electrical stimulation (2 Hz) mainly promotes the release of enkephalin and endorphin, whereas high-frequency pulsed electrical stimulation (100 Hz) mainly increases the release of dynorphin [40].

In addition, the even shorter pulse width can affect the recovery of muscle fibers [41]. The typically used pulse width of TENS device in the market varies from 0 to 500 us [42]. Combining the relevant standards of the stimulation pulse width and the needs of different clinical patients, the system needs to set a wider dynamic adjustment range.

Even though the selection of acupuncture points is mainly determined by the meridian theory of traditional Chinese medicine, the measurement of results, and the design of TENS parameters are based on modern biomedical research. During treatment, the estimated value of the patients' tolerance should be lowered, and different intensities and frequencies should be selected according to different conditions for pulse stimulation.

TABLE I
SYSTEM TECHNICAL INDICATORS

Indicator	Range	Adjustment step
Intensity/V	0-100	1
Frequency/Hz	0-100	1
pulse width/μs	0-500	100

The main technical indicators of the system are shown in Table I.

III. CIRCUIT BLOCKS DESIGN

A. Signal Control Module

STM32L152RCT6, a 32-bit microcontroller with high performance and low power consumption, suitable for electronic medical products and wearable devices, is used as the main control chip in the system. The operating frequency is achieved by an 8 MHz external crystal oscillator through an internal frequency multiplier circuit. The voltage regulator chip MCP1700T and the rechargeable lithium-polymer battery collectively provide a 3.3 V stable voltage for the wearable circuit, which enhances the accuracy and stability of the circuit. A TP4056 power management chip is used to provide power for the lithium battery and to indicate the power status intuitively.

B. Boost and Voltage Feedback Circuit

The boost and voltage feedback circuit is the core part of the dedicated analgesic circuit and provides stable treatment intensity. Conventional TENS products with transformers are bulky and unsuitable for wearing. The boost circuit strategy proposed in this paper uses in-line color ring inductors to improve circuit efficiency, an FMMT497A transistor as a switch tube, a UF4007 fast recovery diode as a freewheeling diode, and a 1608 packaged 10 μF ceramic capacitor as a charging capacitor. This circuit has few components and adopts a full-chip package, which can be miniaturized and wearable. The boost circuit converts a 3.3 V power supply to a 0-100 V adjustable treatment voltage.

In addition, the impedance of the skin to the electrode changes according to the frequency. For 1 cm^2 skin, the impedance is approximately 200 KΩ at 1 Hz and only approximately 200 Ω at 1 MHz [43]. When using a dry electrode that does not contain conductive paste, such as a metal wire electrode, the contact resistance of the electrode-skin will be greater, up to several megaohms to tens of megaohms. This study discusses the establishment of compensation by adding a feedback circuit when a slight change in skin impedance with frequency affects the treatment voltage.

The boost circuit has a proportion-integral-derivative feedback control mechanism to ensure the stability of the current intensity through the human skin. A feedback circuit is added to the boost circuit, and the output voltage is recorded and fed back in real time to form a closed-loop control system.

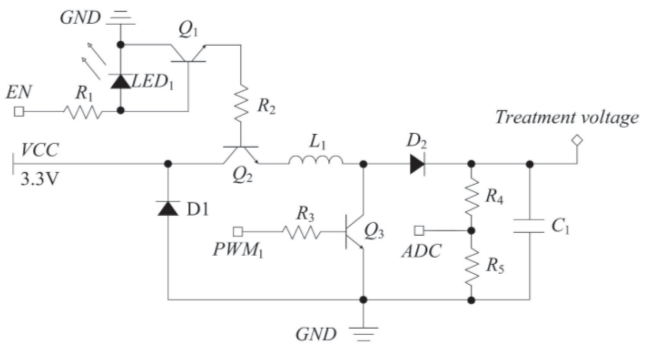

Fig. 4. Schematic diagram of the boost and feedback circuits.

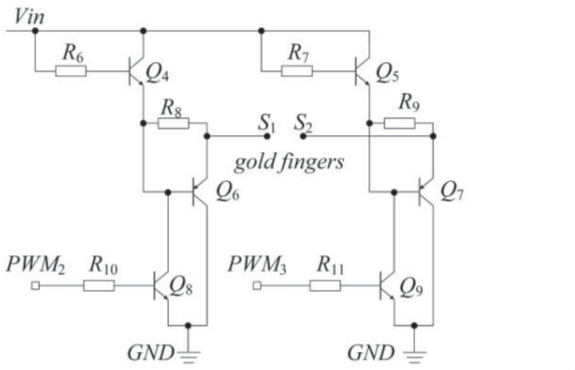

Fig. 5. Schematic diagram of bipolar conversion circuit.

The circuit overcomes the interference of the patients' skin impedance during treatment and continuously outputs a stable treatment voltage, which has high accuracy and safety. The boost and feedback circuits are shown in Fig. 4.

When the stimulation is enabled, the main chip generates a PWM_1 wave with a frequency of 32 kHz and a duty cycle of 0-80%, which controls the turning on and turning off of the transistor Q_3. When Q_3 is turned on and the Schottky diode D_2 is reverse biased, the circuit converts electrical energy into magnetic energy and stores it in the inductor L_1. When Q_3 is disconnected and D_2 is forward biased, the power supply and input power supply the load together and charge the output capacitor C_1 because the voltage of the inductor L_1 cannot change suddenly. When Q_3 continuously switches on and off, the input voltage is pumped to the required treatment voltage through the current holding effect of the inductor L_1, the freewheeling effect of the Schottky diode D_2 and the charging and discharging effect of the output capacitor C_1.

According to the design requirements, the treatment voltage is adjusted to a value between 0 and 100 V. The energy and control formula is established by the discontinuous working mode of the boost topology circuit. The power transferred from the inductor L_1 to the load when Q_3 is off (assuming the transfer efficiency is 100%) is calculated as follows

$$P_L = \frac{1/2L_1(I_P)^2}{T} \tag{1}$$

$$I_P = \frac{V_{dc}T_{on}}{L_1} \tag{2}$$

where I_P is the peak current of L_1, L_1 is the inductance, T is the total working time, $V_{\rm dc}$ is the DC supply voltage of 3.3 V, and T_{on} is the pulse width time. When Q_3 is off, the DC power supply also provides current to the load through L_1 and Q_2 for a total power delivered to the load is as follows

$$P_t = \frac{{V_{dc}}^2 T_{on}}{2TL_1}\ (kT)\ = \frac{{V_o}^2}{R_o} \tag{3}$$

$$V_o = V_{dc}\sqrt{\frac{kR_oT_{on}}{2L_1}} \tag{4}$$

where $V_{\rm o}$ is the treatment voltage, and $R_{\rm o}$ is the sum of loads R_4 and R_5 (assumed to be 3 KΩ). The value of k is 0.8 such that the circuit is in the discontinuous working mode. The resistances R_4 and R_5 constitute the sampling circuit. The sampling circuit is compared with the set voltage after the A/D conversion of the leading chip; therefore, the duty cycle of the PWM_1 wave is adjusted dynamically. The treatment voltage is close to the set voltage, resulting in a high level of accuracy and safety of the output voltage. Transistors Q_1 and Q_2 form enable terminals, and EN is connected to the I/O port of the main control chip. When the system is in a nontreatment state, the I/O port is low, and the boost circuit is isolated from the power supply and turned off. When the I/O port is high, the power is turned on, and the boost circuit is enabled.

C. Bipolar Conversion Output Circuit

During electrical stimulation therapy, the signals used mainly include the unidirectional pulsed electrical stimulation signal and bidirectional pulsed electrical stimulation signal. However, the long-term stimulation of unidirectional high-voltage electricity can easily cause tolerance and polarization of human skin [44]. Furthermore, the severity of electrochemical damage to nerve fibers caused by unidirectional pulse stimulation is higher than that caused by bidirectional pulse stimulation. The system uses a bipolar conversion output circuit composed of MMMBT5551 and MMMBT5401 transistors to output symmetrical bidirectional rectangular pulses, which reduces the tolerance and polarization response. The bipolar conversion output circuit is shown in Fig. 5.

In the schematic diagram of the bipolar conversion circuit, the current-limiting resistors R_8 and R_9 were added to prevent the short circuit between the electrical stimulation electrodes from causing excessive current and harming the user. The main control chip generates two *PWM* waves with the same frequency, the same pulse width, and a 180° phase difference—namely PWM_2 and PWM_3. The bipolar conversion circuit is used to output bidirectional electrical pulses. When PWM_2 is high and PWM_3 is low, current flows from *Vin* through Q_5, R_9, electrode S_2, electrode S_1, and Q_6 to the ground. Conversely, when PWM_3 is high and PWM_2 is low, current flows from *Vin*, Q_4, R_8, electrode S_1, electrode S_2, and Q_7 to the ground. When both PWM_2 and PWM_3 are low, the voltage across the electrodes is the same,

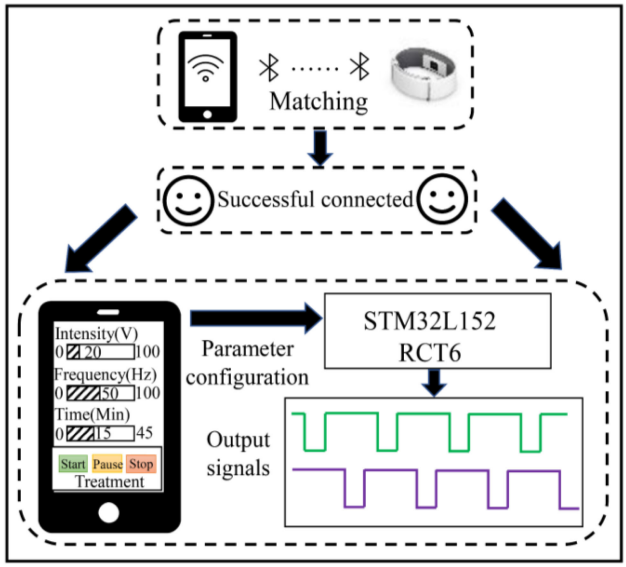

Fig. 6. Wireless signal module flow chart.

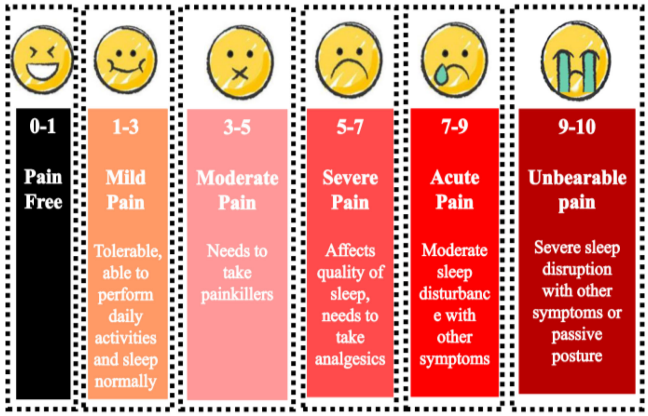

Fig. 7. Pain assessment scale.

and no current flows. One end of the stimulation electrode pair is connected to S_1 and S_2, and the other end is connected to the surface of the human skin to provide electrical stimulation. The configuration formula of the electrical stimulation pulse frequency is as follows

$$f = \frac{1}{T_{out}} = \frac{T_{clk}}{2 \times arr \times psc} \tag{5}$$

where T_{clk} is the input frequency of the timer, *arr* is the preload value of the timer, and *psc* is the prescaler value of the timer.

D. Wireless Communication Module and Pain Assessment Scale

The wireless communication module designed for this system is used for data transmission with intelligent mobile terminals, including Bluetooth communication and parameter configuration. The communication module uses the world's smallest Bluetooth Low Energy serial port transmission module launched by Hongjia Electronics. The size of the Bluetooth module is 0.5 cm $\times$ 0.62 cm, and the maximum power consumption is 280 μA, which effectively minimizes the size and power consumption of the wearable device.

The flow of information through the wireless communication module is shown in Fig. 6. Before treatment, the intelligent terminal and the microprocessor should be wirelessly connected via Bluetooth. After the Bluetooth connection is successful, the intelligent terminal enters the parameter configuration interface. The wireless communication module transmits the instructions of the processing parameter configuration, starts the processing, stops the processing, and suspends the processing to the microprocessor through Bluetooth. Therefore, the corresponding intensity and frequency of the electrical pulses are output.

Pain assessment is fundamentally important for the management of pain. Optimal management requires a tailored approach, support for self-management, and a review of the treatment outcomes. The score scales are often used in clinical pain measurement and evaluation, including the visual analog scale (VAS), the digital expression scale, a pain questionnaire, pain descriptors, and descriptive area scales, among which VAS is the most widely adopted self-assessment method [45]. This system combines the Changhai pain scale and the others to design a custom pain assessment scale with visual analog, digital expression, and pain descriptive text based on the intelligent terminal platform to evaluate pain before and after treatment, as shown in Fig. 7. The expression from smiling to crying is a facial expression of the degree of pain. The smile on the far left means that there is no pain at all, and the cry on the far right means that the pain is at the top and cannot be tolerated. For infants or patients who are unable to communicate, it may be difficult to evaluate pain through numbers and textual descriptions of symptoms [46]. It can be evaluated by a picture scoring method with different facial expressions. The value of the pain assessment scale is used as an indicator for the effectiveness of treatment in this study. The pain scale is divided into ten levels. Before and after treatment, the user can subjectively assess the degree of pain according to the prompts on the pain assessment scale. A statistically significant reduction in the numerical score of pain at any time throughout the study is considered a favorable result, and the effectiveness of interventions is qualitatively assessed. In addition, the intelligent terminal records and stores the evaluation results and dates for future pain management and historical data.

IV. Experiments and Results

A. Participants

To verify the analgesic effect of the bracelet, experimental pain-inducing schemes were designed and implemented, and the effectiveness of the system was tested through different pain assessment methods.

Healthy, painless adult volunteers who did not take medication were recruited from college students, and patients with pacemakers, tumors, diabetes, peripheral vascular disease, local skin infections, or limb pain were excluded. Twenty healthy volunteers (10 men and 10 women) participated in the study.

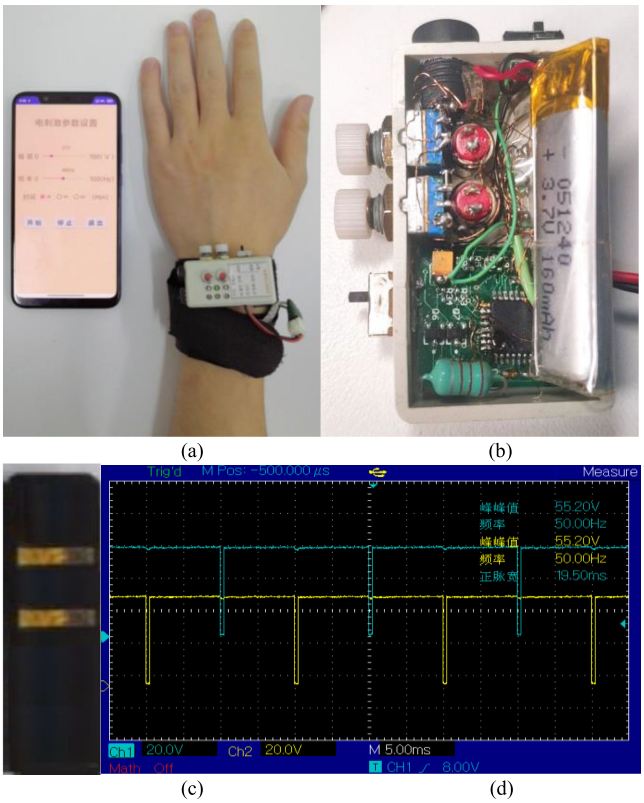

Fig. 8. Schematic diagram of experimental setup and output signal. (a) Principle prototype. (b) Internal layout. (c) Gold finger electrode embedded on flexible band. (d) Output pulses.

The setting and data collection of the subjects were: age 23.7 ± 1.59 (years old), height 168.9 ± 6.68 (cm), weight 57.1 ± 9.39 (Kg). The study was approved by the Ethics Committee of ChiRCT, and participants were required to sign a written informed consent.

B. Apparatus

Fig. 8(a) shows the photography of the proposed intelligent analgesic bracelet. The flexible band is made of velcro fabric and the length is 25.5 cm to cover the six zones of the wrist. The gold finger electrodes are based on pure copper, with a thin composite coating on the outer surface. An intelligent terminal is suitable for the Android operating system. One PCB with a size of 4.5 cm × 2.4 cm was used as shown in Fig. 8(b). The PCB is sealed in a customized box with a size of 4.8 cm × 2.8 cm. The customized box can be folded on the outside of the band. Fig. 8(c) shows the positional relationship between the flexible band and the gold finger electrodes. The distance between the electrodes is 4.2 cm. The actual output pulse is displayed on the oscilloscope as shown in Fig. 8(d).

C. Statistical Analysis

All quantitative variables were presented with means ± standard deviation. Paired-sample T-test was used for statistical analyses. All test results yielding P-value < 0.05 were considered statistically significant, and analyses were conducted by using SPSS statistical software (Version 23).

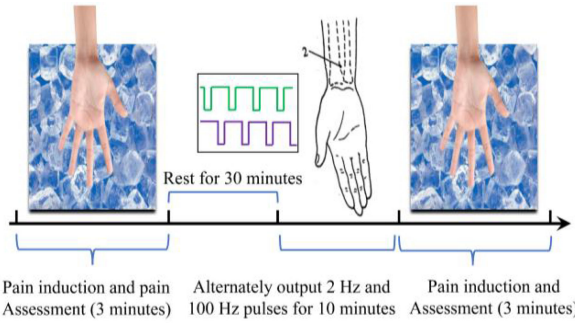

Fig. 9. Subjective pain assessment experiment of cold stimulation-induced pain. This experiment used ice water to induce pain in subjects and established a pain model.

D. Experimental Evaluation of Analgesic Bracelet

The subjects rested reasonably without any pain or discomfort the day before the experiment. All participants were instructed to refrain from caffeine, nicotine, alcohol, and strenuous exercise for 4 hours before the experiment. The data were collected in the university's research laboratory, and the experiments were conducted in a sound-attenuated and electrically shielded room.

1) Customized Subjective Pain Assessment Scale Experiment: Twenty healthy adults (22 to 25 years old) were selected as experimental subjects. The subjects separated the fingers of their left hands and exposed them to an ice water mixture at 0°C for 3 minutes to induce pain first. During this period, the subjects independently assessed and recorded their pain levels according to the custom pain assessment scale every 30 seconds. If the subject felt unbearable pain during the experiment, the experiment could be ended immediately. The subjects rested in a quiet environment for 30 minutes after pain was induced by cold stimulation [47], [48]. The subjects then wore the bracelet for pain treatment. According to the WAA clinical experience, the upper 2 area was selected as the treatment site, which is located in the middle of the palm surface between the two most prominent palmar longus tendons and the flexor carpi radialis tendons. The subjects placed the two gold fingers of the bracelet in the corresponding area and then turned on the bracelet by pressing the button. The treatment parameters were set through the Bluetooth data transmission of the intelligent terminal or the knobs and buttons of the bracelet. The treatment intensity was increased from 0 V and adjusted to the maximum intensity that the subjects could bear without pain. The bracelet output pulses of 2 Hz and 100 Hz in sequence every 1 minute, and the treatment lasted for 10 minutes. After that, the subjects placed their left hands with all five fingers extended into the icewater mixture at 0°C for 3 minutes to induce sharp pain again. While pain was induced, the electrical stimulation output therapy was maintained. The subjects evaluated the pain levels they experienced according to the pain assessment scale every 30 seconds. The experimental design is shown in Fig. 9.

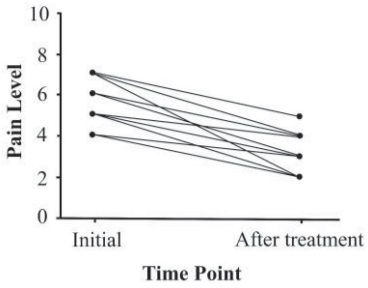

Fig. 10. Evolution of pain (induced by ice water) before and after treatment for subjects. Pain level was estimated using customized subjective pain assessment scale (N = 20).

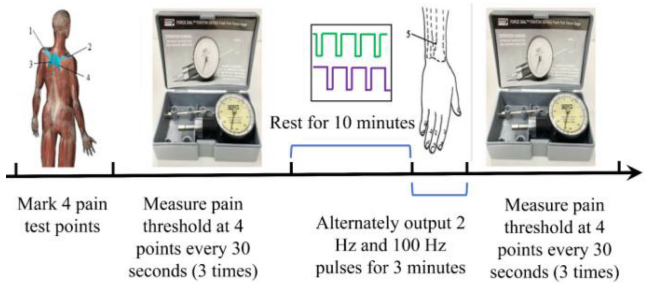

Fig. 11. Objective pain assessment experiment for pain induced by a hand-held dolorimeter. 1- the left supraspinatus, 2- the right supraspinatus, 3- the left rhomboid, and 4- the right rhomboid.

TABLE II
RESULTS OF COMPARATIVE ANALYSIS OF PAIN LEVELS BEFORE AND AFTER TREATMENT (INDUCED BY ICE WATER)

Time	Pain level	Paired t	P-value
Before treatment	5.75±0.85	19.494	<0.001
After treatment	3.75±0.85		

The evolution of the subjects' pain levels before and after analgesia treatment is shown in Fig. 10. After the initial experimental pain induction, the pain levels of 20 subjects concentrated in 4-7. The pain levels induced by the second experimental pain after treatment were concentrated in 2-5. A comparative analysis of the data before and after treatment showed that the pain levels of 20 subjects were significantly reduced. Specifically, there were 2-3 levels of pain reduction for each subject, and even five levels for others. To enhance the credibility of the data, a paired-sample T-test was performed. The results show that the variables follow a normal distribution, as shown in Table II. Since the value of $P < 0.001$, the data before and after treatment have extremely significant differences.

For the experimental hand pain induced by ice water, using the frequency conversion pulses (2 Hz/100 Hz) produced by the bracelet to simulate WAA has a significant effect on analgesia in the specific area, and the difference is statistically significant. It is worth mentioning that although clinical pain and experimental pain cannot be directly compared, experimental pain has been used to study the pathophysiology of pain and to assess the effect of pain relief under controlled conditions. Clinically different parameters still have preferred parameters for different properties. For neuropathic pain, low frequency (2 Hz) or frequency conversion (2/100 Hz) is used in treatment. High frequency (100 Hz) or frequency conversion (2/100 Hz) are used in the treatment of chronic inflammatory pain. The frequency of cancer pain treatment can be high (100 Hz), low frequency (2 Hz), or frequency conversion (2/100Hz) [49]. Therefore, this paper uses frequency conversion (2/100 Hz) output in the test to evaluate the analgesic effect. Frequency conversion (2/100 Hz) electrical pulses can promote the release of enkephalins, endorphins, and dynorphins in the body during treatment, thereby producing analgesic effects. This is a hypothesized explanation of the analgesic mechanism of this bracelet system based on the previously published results of electroacupuncture studies. The specific analgesic mechanisms of this bracelet system should be further investigated.

However, the customized pain assessment scale used in this experiment is subjective. The pain level is only based on the subjects' description and cognition, which is closely related to their mental state. This paper proposes another objective pain evaluation experiment that combines pain induction and evaluation to measure the analgesic effect of the bracelet.

2) Objective Pain Assessment Scale Experiment: To further determine the effectiveness of the bracelet in analgesia, we used a hand-held dolorimeter (FDK20, Wagner Instruments, USA) to induce pain and assess the pain threshold of the subjects. Fifteen healthy adults (8 men and 7 women) were selected as the subjects. One end of the instrument was a pressure rod with a rubber pad, and the other end was a circular pressure scale with a measuring range of 1 to 10 kg/cm^2. In this experiment, the supraspinatus and rhomboid muscles associated with periarthritis, which are the most commonly experienced pain areas in healthy people, were selected as the pain induction points. Before the test, the four test points on the left and right supraspinatus and the left and right rhomboid muscles were marked with markers.

The experimental design is presented in Fig. 11. We used a hand-held dolorimeter to slowly apply increasingly vertical pressure to the test points on the subjects first. During this period, the subjects immediately gave a verbal signal when they felt pain, and the meter reading at this time was recorded. The test was repeated three times at each test point with an interval of 30 s between each test. Second, the subjects rested in a quiet environment for 10 minutes and then used the bracelet to perform analgesic treatment for 10 minutes. Based on clinical experience related to WAA, the upper 5 area of the shoulder was selected as the site for the treatment of periarthritis, and this area was located in the center of the dorsal wrist at the midpoint between the radius and ulna. The treatment intensity was increased from 0 V and adjusted to the maximum intensity that the subjects could bear without pain. At the same time, the bracelet output pulses of 2 Hz and 100 Hz in sequence every 1 minute, and the treatment lasted for 3 minutes. After 3 minutes of treatment, the

TABLE III
RESULTS OF THE COMPARISON OF THE PAIN THRESHOLD AT FOUR TEST POINTS BEFORE AND AFTER TREATMENT (KG/CM^2)

Variable	Pain level	Paired t	P-value
Left supraspinatus (before treatment)	3.14±0.71	-3.348	0.005
Left supraspinatus (after treatment)	3.86±0.92		
Right supraspinatus (before treatment)	3.16±0.62	-3.631	0.003
Right supraspinatus (after treatment)	3.88±0.85		
Left rhomboid (before treatment)	2.84±0.42	-4.331	0.001
Left rhomboid (after treatment)	3.81±0.94		
Right rhomboid (before treatment)	2.96±0.51	-3.937	0.001
Right rhomboid (after treatment)	3.78±0.60		

pain threshold at the four test sites was measured again. Three repeated measurements at each test location were recorded, and the average value was used for analysis. The interval between measurements was 30 seconds. The electrical stimulation output of the treatment was maintained during the trial.

Table III shows the comparison results of the pain levels at the four test points before and after treatment. The pain threshold of the left supraspinatus and the right supraspinatus is the same, but there is a slight difference between the left and right rhomboid muscles before treatment. However, the supraspinatus has a higher pain threshold and pain tolerance than the rhomboid muscles. Focusing on the pain threshold after treatment, the left supraspinatus and the right supraspinatus still maintained consistent tolerance, and the small gap between the left rhomboid muscle and the right rhomboid muscle tended to narrow. Through the paired sample T test of the pain threshold of the four groups of muscle test points before and after treatment, the data of all variables obey the normal distribution and the difference is statistically significant. There were significant differences in each group before and after treatment, and the subjects' pain threshold was significantly higher than before treatment. Among them, the $P < 0.001$ of the left and right rhomboid muscles has extremely significant differences before and after treatment. In the experiment, the slight difference in the treatment effect of the test points on the four muscles is mainly related to the subjects' muscle mass and the accuracy of the test point marking position. This bracelet can still significantly relieve pain after the new pain induction and evaluation experiment.

In summary, whether it is using a customized pain assessment scale to test the pain level, or using a pressure pain instrument to evaluate the pain threshold, the intelligent bracelet based on the WAA can be worn on the wrist to increase the pain threshold and reduce the pain level after treatment. Additional research and experiments are needed to explore this system further.

V. CONCLUSION

This paper proposes a multifunctional, flexible, wearable intelligent analgesic bracelet based on the WAA theory. The smart bracelet combines modern physical electrical stimulation therapy with traditional Chinese medicine WAA theory, and replaces the invasive treatment of WAA with pulses of characteristic parameters.

Currently widely used analgesia systems include multifunctional stimulator (TS-6000) [50] and transcutaneous electrical nerve stimulator (KD-2A) [51], most of which use bulky transformer enhancement solutions and cannot be worn. This bracelet uses the boost topology circuit principle and full-chip components instead of the traditional boost solution, which effectively reduces the volume and weight of the bracelet to make it wearable. In addition, the closed-loop control method effectively improves the output accuracy of the treatment voltage, and makes the treatment pulse between 0-100V and the pulse frequency between 0-100Hz continuously adjustable. The theory of traditional Chinese medicine is implemented with the help of devices. All the pain information of the body can be mapped on the wrist and ankle one by one, realizing holographic mapping for analgesia. The patients only need to wear the wristband on the wrist or ankle, and rotate the electrodes to the corresponding area guided by the WAA to treat the pain of different organs of the body. The bracelet is equipped with intelligent terminal applications to achieve visual and precise control and improve user experience. A large amount of user treatment information can be stored on the cloud storage terminal for later data statistics and analysis, to achieve in-depth data mining, and provide patients with a traceability therapy process. Since the bracelet acts on the human body through the electrode directly, a current-limiting resistor is added to the circuit to limit the output current within a safe range, avoiding abnormally large currents and improving safety. The design fully complies with the specifications in YY0607-2007 "Medical Electrical Equipment Part 2: Nerve and Muscle Stimulator Safety Special" and GB9706.1-2007 "Medical Electrical Equipment Part 1: General Requirements for Safety".

In general, we observed a highly beneficial effect after the analgesic bracelet. We saw a considerable reduction in VAS. This led to an increase in the patients' pain threshold, positively influencing voluntarily and spontaneously conducted treatments. The results may provide evidence of a potential alternative treatment for chronic pain and evidence-based proof for the analgesic effect of WAA. To our knowledge, this is the first description of the electronic wearable analgesic device based on the WAA theory. Our study also offers valuable guidelines for the implementation of a future study addressing this research question. Naturally, our work has limitations and needs further improvement. In the future, we will invest more time and energy in the following directions:

1) Perform clinical trials in large-scale populations and patients. While confirming the analgesic effect, it is also possible to study the influence of different parameters on the analgesic effect based on big data samples.

2) An impedance detection circuit and current detection circuit should be added to reduce the nonlinear change in human body impedance caused by the frequency change to further ensure the safety of use.
3) This system is developed only for the Android operating system. Given that iOS is a more widely used system, a supporting application for the iOS system should be designed.

REFERENCES

[1] S. Vaillancourt *et al.*, "Combining transcutaneous electrical nerve stimulation with therapeutic exercise to reduce pain in an elderly population: A pilot study," *Disabil. Rehabil.*, vol. 21, no. 2, pp. 1–8, 2019.

[2] A. Y. Fan *et al.*, "Acupuncture's role in solving the opioid epidemic: Evidence, cost-effectiveness, and care availability for acupuncture as a primary, non-pharmacologic method for pain relief and management-white paper 2017," *J. Integr. Med.*, vol. 15, no. 6, pp. 411–425, Nov. 2017.

[3] B. Magrum *et al.*, "Combating the opioid epidemic in acute general surgery: Reframing inpatient acute pain management," *J. Surg. Res.*, vol. 251, pp. 6–15, Jul. 2020.

[4] E. B. Rosero and G. P. Joshi, "Preemptive, preventive, multimodal analgesia: What do they really mean," *Plast. Reconstr. Surg.*, vol. 134, no. 4, pp. 85S–93S, Oct. 2014.

[5] D. J. Engen *et al.*, "Evaluating efficacy and feasibility of transcutaneous electrical nerve stimulation for postoperative pain after video-assisted thoracoscopic surgery: A randomized pilot trial," *Complement. Ther. Clin. Pract.*, vol. 23, pp. 141–148, May 2016.

[6] R. Taghavi *et al.*, "Application of electroacupuncture for postoperative pain management after total knee arthroplasty: A study protocol for a single-blinded, randomised placebo-controlled trial," *BMJ Open*, vol. 9, no. 4, pp. e026084–e026090, Jun. 2019.

[7] S. S. Li *et al.*, "Electroacupuncture for postoperative pain after nasal endoscopic surgery: Study protocol for a pilot randomized controlled trial," *Trials*, vol. 21, no. 1, pp. 163–171, Feb. 2020.

[8] J. Xu, F. Q. Zhang, J. Pei, and J. Ji, "Acupuncture for migraine without aura: A systematic review and meta-analysis," *J. Integr. Med.*, vol. 16, no. 5, pp. 312–321, Sep. 2018.

[9] A. Y. Fan *et al.*, "Discussions on real-world acupuncture treatments for chronic low-back pain in older adults," *J. Integr. Med.*, vol. 17, no. 2, pp. 71–76, Mar. 2019.

[10] U. O. Abaraogu and C. S. Tabansi-Ochuogu, "As acupressure decreases pain, acupuncture may improve some aspects of quality of life for women with primary dysmenorrhea: A systematic review with meta-analysis," *J. Acupunct. Meridian Stud.*, vol. 8, no. 5, pp. 220–228, Oct. 2015.

[11] A. Y. Fan *et al.*, "Acupuncture price in forty-one metropolitan regions in the United States: An out-of-pocket cost analysis based on okcopay.com," *J. Integr. Med.*, vol. 17, no. 5, pp. 315–320, Sep. 2019.

[12] A. Y. Fan and S. Faggert, "Distribution of licensed acupuncturists and educational institutions in the United States in early 2015," *J. Integr. Med.*, vol. 16, no. 1, pp. 1–5, Jan. 2018.

[13] L. Tan *et al.*, "Effect of electroacupuncture at different acupoints on the expression of NMDA receptors in ACC and colon in IBS rats," *Evid. - Based Complement Altern. Med.*, vol. 2019, pp. 1–12, 2019.

[14] M. L. Reeves, C. Chotiyarnwong, K. P. S. Nair, M. Slovak, and T. J. Healey, "Caregiver delivered sensory electrical stimulation for post stroke upper limb spasticity: A single blind crossover randomized feasibility study," *Health Technol.*, vol. 10, no. 5, pp. 1265–1274, Sep. 2020.

[15] A. O. Abass, A. R. Alli, O. M. Olagbegi, C. J. Christie, and S. O. Bolarinde, "Effects of an eight-week lumbar stabilization exercise programme on selected variables of patients with chronic low back pain," *Bangladesh J. Med. Sci.*, vol. 19, no. 3, pp. 467–474, Jul. 2020.

[16] V. Malik, U. Kiran, S. Chauhan, and N. Makhija, "Transcutaneous nerve stimulation for pain relief during chest tube removal following cardiac surgery," *J. Anaesthesiol. Clin. Pharmacol.*, vol. 34, no. 2, pp. 216–220, Apr. 2018.

[17] H. R. Ranga, S. Yadav, D. K. Garg, and P. Garg, "Comparative evaluation of transcutaneous electrical nerve stimulation (tens) v/s non-steroidal anti-inflammatory drugs (NSAIDs) for postoperative pain management in open cholecystectomy," *J. Evol. Med. Dent. Sci.*, vol. 5, no. 47, pp. 3072–3075, Jun. 2016.

[18] S. Kayman-Kose, D. T. Arioz, H. Toktas, G. Koken, M. Kanat-Pektas, and M. Kose, "Transcutaneous electrical nerve stimulation (tens) for pain control after vaginal delivery and cesarean section," *J. Matern. - Fetal Neonat. Med.*, vol. 27, no. 15, pp. 1572–1575, Oct. 2014.

[19] M. P. Da Silva, R. E. Liebano, V. A. Rodrigues, L. E. F. Abla, and L. M. Ferreira, "Transcutaneous electrical nerve stimulation for pain relief after liposuction: A randomized controlled trial," *Aesthet. Plast. Surg.*, vol. 39, no. 2, pp. 262–269, Apr. 2015.

[20] Y. Chen, X. Zhang, Y. Zhu, Y. Jia, H. Wang, and Y. Liu, "Systematic review of three electrical stimulation techniques for rehabilitation after total knee arthroplasty," *J. Arthroplast.*, vol. 33, no. 7, pp. 2330–2337, Jul. 2018.

[21] P. E. Gonzalez, N. M. Novoa, and G. Varela, "Transcutaneous electrical nerve stimulation reduces post-thoractomy ipsilateral shoulder pain. a prospective randomized study," *Arch. Bronconeumol.*, vol. 51, no. 12, pp. 621–626, Dec. 2015.

[22] W. W. Peng *et al.*, "Neurobiological mechanisms of TENS-induced analgesia," *Neuroimage*, vol. 195, pp. 396–408, Jul. 2019.

[23] C. G. Vance, D. L. Dailey, B. A. Rakel, and K. A. Sluka, "Using tens for pain control: The state of the evidence," *Pain Manage.*, vol. 4, no. 3, pp. 197–209, May. 2014.

[24] M. E. D. J. Agripino, L. V. Lima, I. F. Freitas, and J. M. Desantana, "Influence of therapeutic approach in the tens-induced hypoalgesia," *Clin. J. Pain*, vol. 32, no. 7, pp. 594–601, Jul. 2016.

[25] R. Melzack and P. D. Wall, "Pain mechanisms: A new theory," *J. Pain*, vol. 5, no. 1, pp. 3–11, Nov. 1996.

[26] P. D. Wall and W. H. Sweet, "Temporary abolition of pain in man," *Science*, vol. 155, no. 3758, pp. 108–109, Jan. 1967.

[27] F. Yange, L. U. Wenliang, M. A. Li, W. Zhitao, and D. Tieli, "Clinical study on transcutaneous electrical nerve stimulation(tens)in the treatment of calcaneodynia," *Chin. J. Pract. Nerv. Dis.*, vol. 21, no. 19, pp. 2184–2189, Nov. 2018.

[28] S. N. Gozani, "Remote analgesic effects of conventional transcutaneous electrical nerve stimulation: A scientific and clinical review with a focus on chronic pain," *J. Pain Res.*, vol. 12, pp. 3185–3201, 2019.

[29] F. MacPherson and L. Colvin, "Transcutaneous electrical nerve stimulation (TENS). research to support clinical practice," *Br. J. Anaesth.*, vol. 114, no. 4, pp. 711–712, Apr. 2015.

[30] X. S. Zhang, C. Q. Ling, and Q. H. Zhou, *Practical Wrist-Ankle Acupuncture Therapy*. Beijing, China: People's Med. Publi. House, 2002.

[31] L. Zhu, W. Chan, K. Lo, T. Yum, and L. Li, "Wrist-Ankle acupuncture for the treatment of pain symptoms: A systematic review and meta-analysis," *Evid. - based Complement Altern. Med.*, vol. 2014, pp. 261709–261709, 2014.

[32] S. Le, Q. I. Chang-Ju, and G. E. Tan, "Clinical observation of wrist-ankle and somatic acupuncture for acute lumbar sprain," *Shanghai J. Tradit. Chin. Med.*, vol. 49, no. 6, pp. 58–59, Jan. 2015.

[33] C. Marra, I. Pozzi, L. Ceppi, M. Sicuri, F. Veneziano, and A. L. Regalia, "Wrist-ankle acupuncture as perineal pain relief after mediolateral episiotomy: A pilot study," *J. Altern. Complement. Med.*, vol. 17, no. 3, pp. 239–241, Mar. 2011.

[34] F. Li, W. Zhang, and Y. Zhao, "Experimental study on the analgesic mechanism of technique wrist ankle needle," *Traditional Chin. Med. Clin. J.*, vol. 23, no. 10, pp. 897–899, 2011.

[35] X. S. Zhang, *Wrist-Ankle Acupuncture*. Beijing, China: People's Mil. Med. Press, 1997.

[36] P. Schier *et al.*, "Model-Based vestibular afferent stimulation: Evaluating selective electrode locations and stimulation waveform shapes," *Front. Neurosci.*, vol. 12, pp. 588–602, Aug. 2018.

[37] R. Ranjandish and O. Shoaei, "A simple and precise charge balancing method for voltage mode stimulation," in *Proc. IEEE Trans. Biomed. Circuits Syst.*, 2014, pp. 376–379.

[38] J. Gregory, S. Tang, Y. Luo, and Y. Shen, "Bio-impedance identification of fingertip skin for enhancement of electro-tactile-based preference," *Int. J. Intell. Rob. Appl.*, vol. 1, no.no. 3, pp. 327–341, Sep. 2017.

[39] R. K. Shepherd and E. Javel, "Electrical stimulation of the auditory nerve: II. Effect of stimulus waveshape on single fibre response properties," *Hear. Res.*, vol. 130, no. 1, pp. 171–188, 1999.

[40] L. L. Cheng, M. X. Ding, C. Xiong, M. Y. Zhou, Z. Y. Qiu, and Q. Wang, "Effects of electroacupuncture of different frequencies on the release profile of endogenous opioid peptides in the central nerve system of goats," *Evid. - based Complement Altern. Med.*, vol. 2012, pp. 457–476, Oct. 2012.

[41] B. M. Doucet, A. Lam, and L. Griffin, "Neuromuscular electrical stimulation for skeletal muscle function," *Yale J. Biol. Med.*, vol. 85, no. 2, pp. 201–215, Jun. 2012.

[42] A. M. Stewart, C. G. Pretty, and X. Chen, *Design and Testing of a Novel, Low-Cost, Low-Voltage, Functional Electrical Stimulator*. Auckland, New Zealand: MESA, 2016, pp. 1–6.
[43] K. Wlodzimierz and D. Sajewicz, "Method for estimating probabilistic models of touch currents and impedance of human body relying on the effects of electric shock," *Arch. Elektrotech. (Warsaw)*, vol. 62, no. 1, pp. 5–13, Jun. 2013.
[44] E. N. Den, N. C. Geene, C. M. Van Rijn, O. H. Wildersmith, and J. M. Oosterman, "Negative expectations facilitate mechanical hyperalgesia after high-frequency electrical stimulation of human skin," *Eur. J. Pain*, vol. 18, no. 1, pp. 86–91, Jan. 2014.
[45] H. Breivik, "Fifty years on the visual analogue scale (VAS) for pain-intensity is still good for acute pain. But multidimensional assessment is needed for chronic pain," *Scand. J. Pain*, vol. 11, no. 1, pp. 150–152, Apr. 2016.
[46] E. J. Gallagher, M. Liebman, and P. E. Bijur, "Prospective validation of clinically important changes in pain severity measured on a visual analog scale," *Ann. Emerg. Med.*, vol. 38, no. 6, pp. 633–638, 2001.
[47] H. Sharini, M. Fooladi, S. Masjoodi, M. Jalalvandi, and M. Pour, "Identification of the pain process by cold stimulation: Using dynamic causal modeling of effective connectivity in functional near-infrared spectroscopy (fNIRS)," *IRBM*, vol. 40, no. 2, pp. 86–94, Mar. 2019.
[48] Y. Zhuo *et al.*, "Brain activation pattern responding to ice-water-induced pain: A functional MRI study," *Neuroimage*, vol. 11, no.no. 5, pp. S753, 2000.
[49] S. J. Zhuang, J. Gong, J. Zhou, and J. Q. Fang, "Progress analgesic effect of experimental parameters on the different electrical stimulation," *J. Zhejiang Chin. Med. Univ.*, vol. 39, no. 12, pp. 913–917, 2015.
[50] Q. J. Li, J. L. Lin, and C. M. Luo, "The clinical effect of the combination of compulsory exercise therapy and neuromuscular electrical stimulation on the rehabilitation of upper limb function in stroke patients with hemiplegia," *Med. Innov. China*, vol. 14, no. 16, pp. 38–41, 2017.
[51] N. Huang and M. A. Chen, "Application of transcutaneous acupoint electrical stimulation combined with cervical plexus block anesthesia in thyroid surgery," *Shandong J. Traditional Chin. Med.*, vol. 39, no. 2, pp. 140–144, 2020.

Ping Shi received the Ph.D. degree in electronic and electrical engineering from Loughborough University, U.K., in 2009. From 2010 to 2012, she was a Postdoctoral Fellow in the area of motor neuroprostheses with Med-X Research Institute, Shanghai Jiao Tong University, China. She is currently an Associate Professor with the Institute of Rehabilitation Engineering and Technology, University Shanghai for Science and Technology, China. Her current research interests include the noninvasive physiological monitoring and development of rehabilitation device.

Jiahao Du received the B.E. degree in biomedical engineering from Nanchang Hangkong University, Nanchang, China in 2018. She is currently working toward the M.E. degree in biomedical engineering with University of Shanghai for Science and Technology, Shanghai, China. Her current research interests include low power integrated circuit design, wearable medical devices and pain assessment.

Fanfu Fang received the Ph.D. degree in clinical medicine from the Second Military Medicine University, Shanghai, China, in 2015. He is currently an Associate Professor with the Department of Rehabilitation Medicine, Changhai Hospital. His research interest focuses on the development of traditional Chinese medicine rehabilitation equipment, rehabilitation exercise and equipment, and clinical research.

Hongliu Yu received the Ph.D. degree in rehabilitation engineering from University of Shanghai for Science and Technology, Shanghai, China, in 2009. He is currently a Professor and the Director with the Institute of Rehabilitation Engineering and Technology, University of Shanghai for Science and Technology, China. He also made contributions in the area of biomedical signal processing and control. His research interest focuses on assistive and rehabilitation technology for people with disabilities, which including intelligent neuroprostheses and rehabilitation robots.

Junwen Liu received the B.E. degree in automation from the Wuhan Institute of Technology, Wuhan, China in 2018. He is currently working toward the M.E. degree in biomedical engineering with University of Shanghai for Science and Technology, Shanghai, China.